Heat Transfer on the Surface of Parallel Plates in the Starting Range

By

Sugao SUGAWARA and Takashi SATŌ

Department of Mechanical Engineering

Synopsis

This research was carried out to make clear the surface heat transfer in the starting range of parallel plates. The laminar heat transfer in the range was theoretically analysed and compared with the experimental results, and the turbulent heat transfer was made clear by various experiments. In the theoretical analysis, the distributions of both velocity and temperature were approximated by the biquadratic equations and the solutions were obtained taking into consideration the fact that the velocity of the main stream accelerates as the boundary layer from the walls grow. Regarding the velocity boundary layer, the results of this solution agree well with that of the Schlichting's exact analysis. Moreover, the theoretical result of the laminar heat transfer agrees also with the experimental results. The experiments were carried out in the passage of parallel plates having flat front edges, and the influences of velocity and the breadth of passage on the length of the starting range and heat transfer were made clear. As the result, it is found that the heat transfer in this case is considerably close to that of the case of a single plate, especially in the range of turbulent boundary layer.

1. Introduction

In spite of the fact that it is an important problem for the heat exchangers and others to make clear the phenomenon of exchanging heat between the plate and flowing fluid while the latter passes through the parallel plates, the researches made public on this problem are few and especially the phenomenon of heat transfer in the starting range has a scarcely been made clear. And yet, in many cases, the starting range covers comparatively long distance; for instance, in the heat exchangers having a comparatively large pitch between the plates or a tube of comparatively large diameter in relation to their length, the starting range often covers the greater part of their total length. At the present, it is considered that the surface heat

transfer in the starting range is approximately equal to that of the fluid flowing along a single plate. But, due to the growth of the boundary layers from the wall, the main flow will be converged and consequently be accelerated and, on the other hand, it is assumed that the boundary layer is pressed. Strictly speaking, therefore, the condition of the boundary layer will not be the same as that of a single plate and, it should be considered that the heat transfer will also be different from that of the case of a single plate.

In this research, the experiment is performed on the passage between the parallel plates, which method is considered convenient to make clear experimentally the condition of the boundary layer; and the condition of boundary layer is ascertained by the distributions of velocity and statical pressure, and the coefficient of the local surface heat transfer is measured. The theoretical analysis is carried out on the laminar heat transfer, and its result is compared with the experimental results. On the other hand, all the experimental researches are conducted solely on the parallel plates having flat front edges for the purpose of clarifying chiefly the conditions of results of the turbulent heat transfer which is concievable to be close to the real condition.

2. Theoretical Analysis on Laminar Heat Transfer[1]

Assuming that the flowing fluid is incompressible and the flow is two dimentional and taking the co-ordinates as shown in Fig. 1, the differential equation of momentum balance in the boundary layer is shown in an integration form as follows :

$$\rho \frac{\partial}{\partial x}\int_0^\delta u^2 dy - \rho u_1 \frac{\partial}{\partial x}\int_0^\delta u dy = \delta u_1 \frac{du_1}{dx} - \nu \left(\frac{\partial u}{\partial y}\right)_{y=0} \tag{1}$$

where, u is the velocity component at y in the x direction, u_1 is the velocity of the main stream at the x position, ρ & ν respectively are the density and the kinematic coefficient of viscosity, and δ is the thickness of a boundary layer.

On the other hand, taking the displacement thickness δ^* into consideration, the following equation is formed :

Fig. 1.

$$u_1(a - \delta^*) = u_0 a \tag{2}$$

where, u_0 is the velocity of the uniform stream before flowing into the row of plates, and a is a half of the breadth of passage between the parallel plates. And

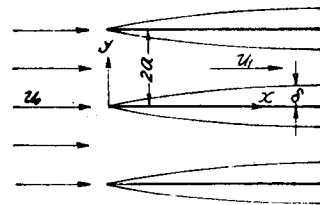$$\delta^* = \frac{1}{u_1}\int_0^\delta (u_1 - u) dy \tag{3}$$

From eq. (2)

$$u_1 = u_0 \left\{ 1 + \left(\frac{\delta^*}{a} \right) + \left(\frac{\delta^*}{a} \right)^2 + \cdots \cdots \right\} \tag{4}$$

Assuming that the form of velocity distribution in the boundary layer is close to that of the case of a single plate, we put it in the Pohlhausen's approximation[2] as follows:

$$\frac{u}{u_1} = 2 \left(\frac{y}{\delta} \right) - 2 \left(\frac{y}{\delta} \right)^3 + \left(\frac{y}{\delta} \right)^4 \tag{5}$$

Applying eq. (5) to eq. (1), we get

$$\frac{337}{630} \delta \frac{\partial u_1}{\partial x} + \frac{74}{630} u_1 \frac{\partial \delta}{\partial x} = \nu \frac{2}{\delta} \tag{6}$$

And, from eq. (5) & eq. (3), we obtain

$$\delta^* = \frac{3}{10} \delta \tag{7}$$

Consequently, adopting approximately the right side of eq. (5) up to the second term, eq. (6) becomes as follows:

$$\left(\frac{\delta}{a} \right)^3 + \frac{370}{411} \left(\frac{\delta}{a} \right)^2 - \frac{1260}{411} \xi = 0 \tag{8}$$

Also, by approximating eq. (5) up to the third term, eq. (9) is obtained.

$$\left(\frac{\delta}{a} \right)^4 + \frac{4110}{1683} \left(\frac{\delta}{a} \right)^3 + \frac{3700}{1683} \left(\frac{\delta}{a} \right)^2 - \frac{126000}{1683} \xi = 0 \tag{9}$$

where,

and

$$\left. \begin{array}{l} \xi = \dfrac{x}{a} \dfrac{1}{R_{ea}} \\[2mm] R_{ea} = \dfrac{u_0 a}{\nu} \end{array} \right\} \tag{10}$$

Therefore, by solving eq. (8) or eq. (9), δ/a is obtained as a function of ξ. The relation between δ/a and ξ is shown in Fig. 2 and the value of ξ at $\delta/a = 1$ is $\xi = 7.534 \times 10^{-2}$ by eq. (9). In this figure, the values shown with ⊙ marks are taken from the Schlichting's exact analysis[3], i. e. we determined δ by taking the value of y at $u/u_1 = 0.995$ in his velocity distribution. Comparing our results with that of the Schlichting's, they agree very well with each other in regard to the thickness of boundary layer. In addition, the chain line shows the Pohlhausen's approximate result in the case of a single plate and the difference between the chain line and the real line increases as ξ becomes larger. Thus, we can determine the
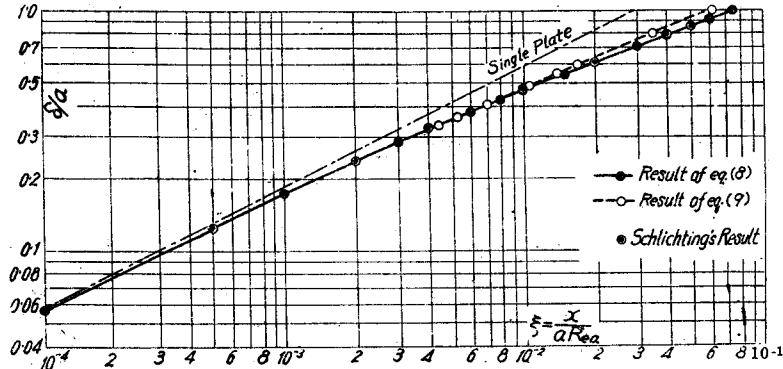
Fig. 2. Thickness of the laminar boundary layer δ of parallel plates.

relation between δ/a and ξ from eq. (8) & (9), and consequently the velocity distribution can be determined by eq. (5). Next, we shall determine the temperature distribution.

The temperature distribution in the boundary layer is assumed similarly to the velocity distribution as follows:

$$\frac{T-T_W}{T_1-T_W} = 2\left(\frac{y}{\delta'}\right) - 2\left(\frac{y}{\delta'}\right)^3 + \left(\frac{y}{\delta'}\right)^4 \tag{11}$$

where, T is the temperature at y, T_1 & T_W are the temperatures of the main stream and the surface of plate respectively, and δ' is the thickness of temperature boundary layer. By integrating the differential equation of heat balance in the boundary layer, the following energy balance equation is obtained:

$$\frac{\partial}{\partial x}\int_0^{\delta'} uTdy - T_1\frac{\partial}{\partial x}\int_0^{\delta'} udy = -k\left(\frac{\partial T}{\partial y}\right)_{y=0} \tag{12}$$

where, $k = \lambda/\rho \cdot c_p$ is the coefficient of thermometric diffusivity and λ, ρ & c_p are respectively the thermal conductivity, density, and specific heat of fluid under constant pressure. Applying eq. (11) and eq. (5) to eq. (12), we have

$$\frac{\partial}{\partial x}\{u_1\delta'F\} = -k\frac{2}{\delta'} \tag{13}$$

where, F is a function of δ'/δ and

$$F = -\frac{2}{15}\frac{\delta'}{\delta} + \frac{3}{140}\left(\frac{\delta'}{\delta}\right)^3 - \frac{1}{180}\left(\frac{\delta'}{\delta}\right)^4$$

Now, putting $\delta'/\delta = c$ and neglecting the smaller terms, we get the following relation.

$$u_0 cF\left\{1+1.035\frac{\delta}{a}+0.2105\left(\frac{\delta}{a}\right)^2-0.1004\left(\frac{\delta}{a}\right)^3\right\}\frac{\partial\delta}{\partial x} = -k\frac{2}{\delta'} \tag{14}$$

From eq. (9) & eq. (14), we oblain

$$c^2 F = -\frac{74}{630} \frac{\varPhi}{\sigma} \qquad (15)$$

where, σ is the Prandtl's number and equals to ν/k, and

$$\varPhi = \frac{1 + 1.667\left(\dfrac{\delta}{a}\right) + 0.9096\left(\dfrac{\delta}{a}\right)^2}{1 + 1.035\left(\dfrac{\delta}{a}\right) + 0.2105\left(\dfrac{\delta}{a}\right)^2 - 0.1004\left(\dfrac{\delta}{a}\right)^3} \qquad (16)$$

Therefore,

$$\frac{2}{15}c^3 - \frac{3}{140}c^5 + \frac{1}{180}c^6 = \frac{74}{630}\frac{\varPhi}{\sigma} \qquad (17)$$

By solving eq. (17),

$$c = \phi/\sigma^{\frac{1}{3}} \qquad (18)$$

where, ϕ is the function of δ/a and σ, however, the influence of σ upon ϕ is very little. The value of ϕ is as shown in Table 1. Thus, when the value of c is known, δ' is determined and the temperature distribution can be calcutated from eq. (11).

Table 1. The value of ϕ.

σ \ δ/a	0.0	0.1	0.2	0.3	0.4	0.5	0.6	0.7	0.8	0.9	1.0
0.73	1.008	1.031	1.054	1.076	1.096	1.117	1.137	1.157	1.177	1.197	1.216
1.0	1.000	1.022	1.044	1.066	1.086	1.106	1.126	1.146	1.165	1.184	1.203
2.0	0.986	1.007	1.028	1.049	1.068	1.088	1.107	1.126	1.144	1.162	1.181
3.0	0.979	1.002	1.022	1.042	1.061	1.079	1.099	1.117	1.135	1.153	1.171
5.0	0.977	0.998	1.018	1.039	1.057	1.077	1.094	1.113	1.132	1.149	1.167

The coefficient of the surface heat transfer α can be determined from the temperature distribution. That is to say:

$$\alpha = \frac{\lambda}{T_1 - T_W}\frac{\partial T}{\partial y}\bigg|_{y=0} = \frac{2\lambda}{\delta'} = \frac{2\lambda}{c\delta} \qquad (19)$$

And the Nusselt's number at the x position is

$$N_{ux} = \frac{\alpha x}{\lambda} = \frac{2x}{c\delta}$$

$$\therefore \frac{N_{ux}}{R_{ea}} = \frac{2}{c}\cdot\frac{a}{\delta}\,\xi = \frac{2}{\phi}\,\sigma^{\frac{1}{3}}\frac{a}{\delta}\,\xi \qquad (20)$$

Since δ/a in this equation is the function of ξ, N_{ux}/R_{ea} is the function of ξ and σ. Fig. 3 shows the relation between $N_{ux}/R_{ea}\cdot\sigma^{\frac{1}{3}}$ and ξ.

On the other hand, the result in the case of a single plate is shown as follows[2].

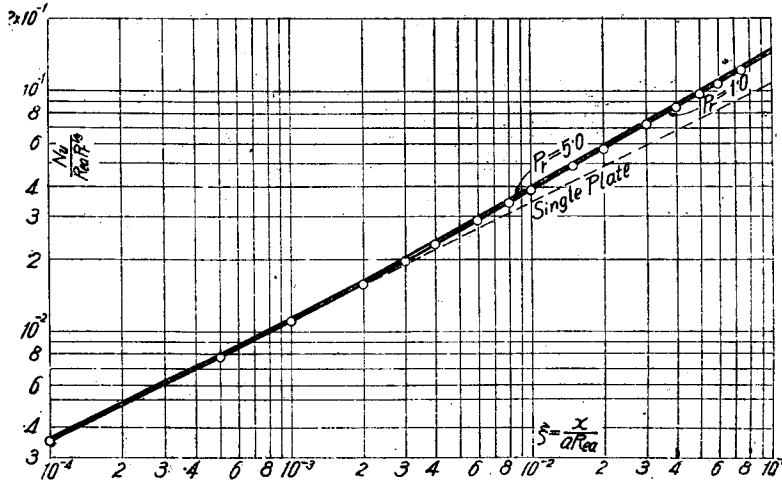$$N_{ux} = 0.343\,\sigma^{\frac{1}{3}}\,R_{ea}{}^{0.5}$$

Fig. 3. Laminar heat transfer of parallel plates.

where,

$$R_{ex} = u_0 x / \nu$$

$$\therefore \frac{N_{ux}}{R_{ea}} = 0.343 \, \sigma^{\frac{1}{3}} \, \xi^{0.5} \qquad (21)$$

A broken line in Fig. 3 shows the relation of eq. (21). Comparing these two results, heat transfer in the laminar boundary layer is better in the case of parallel plates than in the case of a single plate, and the difference between them increases as ξ increases. The cause of this difference, we consider, may be attributable to the fact that, in the case of parallel plates, the main stream is accelerated with the growth of the boundary layer and, as the result, the velocity boundary layer is pressed and its thickness becomes thinner than in the case of a single plate; at the same time, the thickness of temperature boundary layer also becomes thinner, thus improving heat transfer.

3. Experimental Research and the Consideration of its Results

The experiemt was carried out on the two types of passages between the parallel plates as shown in Fig. 4. The parallel plates of type I is considered important for the heat exchangers of cocurrent flow type or countercurrent flow type, and of type II, in which every other flow passage of type I is shut as shown in Fig. 4, can be considered
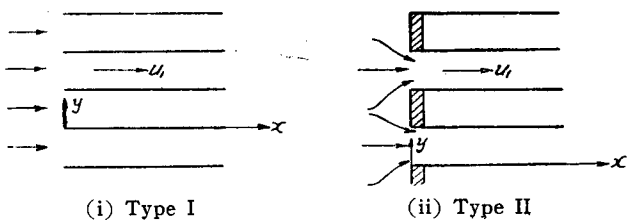

(i) Type I   (ii) Type II

Fig. 4,

as the fundamental for the heat exchangers of cross flow type. The parallel plates are placed in air flow, and the measurement of the coefficient of local surface heat transfer on the parallel plates of type I is done while the plates are cooled by air[4]. In other words, the plates are heated by hot air first and the temperature of plates reaches certain constant value; then cold air is sent to the heated plates and, at the same time, taking of the measurement commences. The coefficient of the local surface heat transfer can be calculated by measuring the time rate of the change of temperature difference between the plates and air at the x position. In addition to the above measurement, the velocity distribution in a boundary layer and the statical pressure distribution in the x direction are measured for the purpose of clarifying the condition of a boundary layer and also ascertaining the influences on its condition of the velocity of fluid and the pitch of plates. Since the above-mentioned method of measuring the coefficient of local heat transfer is not applied in the case of type II, a comparision was made between type I and II from the results obtained of velocity distribution and statical pressure distribution.

The thickness of the plate used in the experiments was 1.5 mm, and its pitch was changed into three steps of 10, 15 & 20 mm, consequentely the breadth of a passage was varied into three steps of 8.5, 13.5 & 18.5 mm, and mean flow velocity was changed also in three steps in the range of 6∼14 m/s. For the parallel plates of type II, experiments were carried out in two cases: one with the round curveture of $r = 4$ mm radius at the flow-in edge and the other without a rounded curveture at the flow-in edge. However, as the greater part of the experiment was carried out for the type I, we put the mark ⅂⌐ for the experiments of the type II to make a distinction.

At first, the results of the distribution of statical pressure and the distribution of velocity will be shown to make clear the condition of the boundary layer.

(i) Statical Pressure Distribution

Some examples of the statical pressure distribution in the x direction are shown in Fig. 5 to Fig. 8. In Fig. 5 & 6, the statical pressure p is taken on ordinate and x on abscissa. And Fig. 7 & 8 show the relation between $(p_0 - p)/\left(\frac{1}{2} \rho u_0^2\right)$ and $\xi = x/(aR_{ea})$, where p_0 is the statical pressure at the front edge (at $x = 0$) and u_0 is the mean velocity. Fig. 5 is the results of $2a = 8.5$ mm and Fig. 6 is that of $2a = 13.5$ or 18.5 mm. In these figures, according to the increase of x the statical pressure decreases abruptly at first, and the decrease becomes gradual and then it once retains a constancy, but the decrease once more becomes remarkable. Since the decrease of statical pressure, in this case, is considered as caused by the growth of the boundary layer, it may well be conceived that the decrease in the first range

is caused by the growth of a laminar boundary layer, and the next remarkable decrease is the consequence of the transition from a laminar boundary layer to a turbulent boundary layer. In Fig. 6, in the case of $2a = 18.5$ mm, the range of the first decrease is very small and it is considered that the greater part is covered by the turbulent boundary layer. These results are made more clear by the expression of Fig. 7 or 8. In these figures, the real line shows the Schlichting's solution for a laminar buondary layer and, therefore, the bound- ary layer, in the range on its line, is in a laminar state. By Fig. 8, a com- parision between the results of the type I and type II can be made and it is conceived that there is no great difference between them. It is thought that the type II, the case of $r = 0$, is rather close to a laminar state, follow- ed by the result of $r = 4$ mm, and the result of the type I is most turbulent.

Fig. 5. Statical pressure distribution (i)

Fig. 6. Statical pressure distribution (ii)
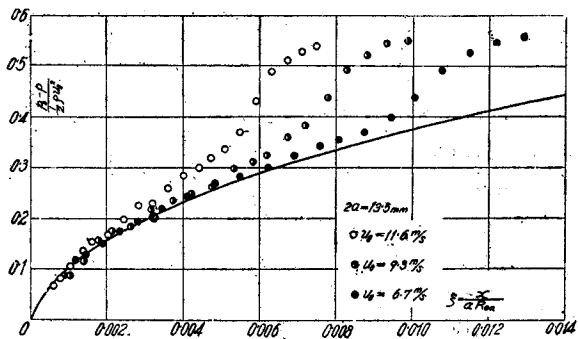
Fig. 7. Statical pressure distribution.
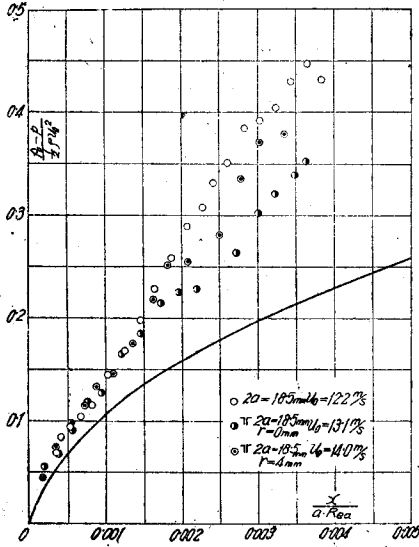
Relation between $(p_0 - p)/\left(\dfrac{1}{2}\rho u_0^2\right)$ and ξ. (i)

(ii) Velocity distribution

Some results of the velo- city distribution are shown in Fig. 9 to Fig. 16. From Fig. 9 to Fig. 12 show the relation between u and y, and from Fig. 13 to Fig. 16 show the relation between u/u_0 and y/δ. By the former

Fig. 8. Relation between $(p_0 - p)/$
$\left(\dfrac{1}{2} \rho u_0^2\right)$ and ξ. (ii)
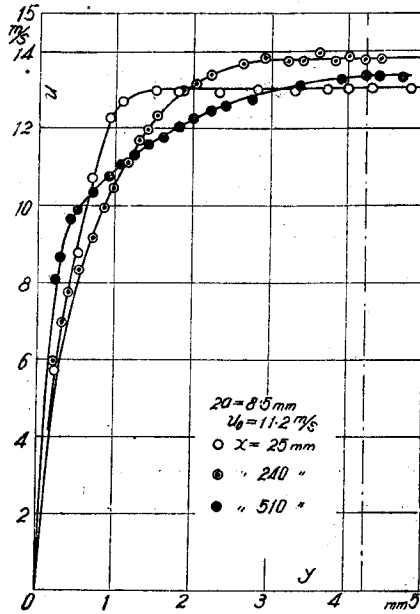
○; TypeI, ◑ & ⊙ ; Type II.

Fig. 9. Velocety distribution in a
boundary layer (i)

four figures, the state of the growth of boundary layer are seen and by the latter four figures, the condition of boundary layer. Fig. 9 shows the distribution of u in the case of $2a = 8.5$ mm and $u_0 = 11.2$ m/s. The chain line shows the center of a passage. In this case, at $x = 510$ mm, there is no existence of main flow seen and it is thought that the starting range has already ended. Fig. 10 shows that of the case of $2a = 13.5$ mm and, in this case, it seems that
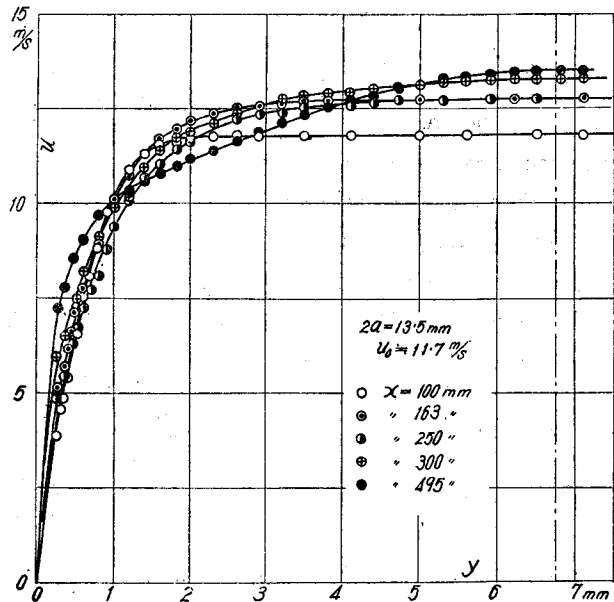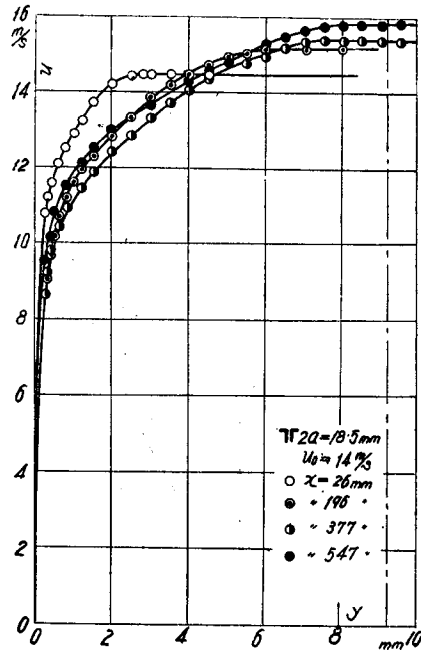
Fig. 10. Velocty distribution (ii)
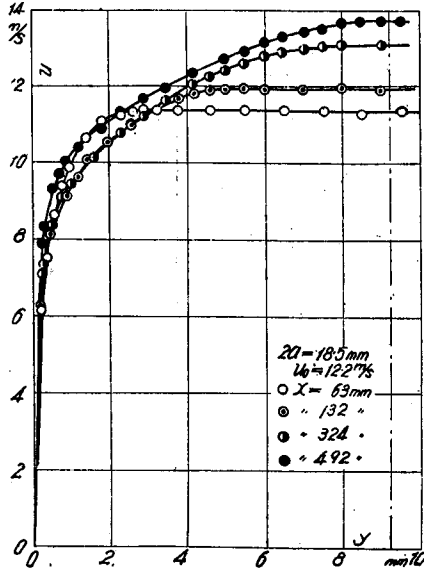
Fig. 11. Velocty distribution (iii)

Fig. 12. Velocity distribution (iv)
(Type II, $r = 4$ mm)

$x = 495$ mm is a point at which the main stream terminaties. Fig. 11 and Fig. 12 are both the results of the case of $2a = 18.5$ mm; Fig. 11 is the case of type I and Fig. 12, the case of type II in which $r = 4$ mm. Comparing these two figures, it is seen that the breadth of the main straem in the case of type II is a little wider than in the case of type I.

In Fig. 13 to Fig. 16, the full line is the Blasius' theoretical result[5] for the laminar boundary layer of a single plate. Fig. 13 & Fig. 14 are both the case of $2a = 13.5$ mm and in Fig. 13 $u_0 = 9.3$ m/s and in Fig. 14 $u_0 = 11.7$ m/s. As is shown by these figures, the laminar boundary layer continues in the longer range corre- sponding to the decrease of the mean velocity. Fig. 15 & Fig. 16 are both the case of $2a = 18.5$ mm and Fig. 15 shows the result of type I and Fig. 16, that of type II. Comparing these two, it appears that the boundary layer is a little more turbulent in the case of type I than in type II.

From the results of statical pressure distribution and velocity distribution, the laminar boundary layer continues longer, corresponding to the smallness of u_0 and $2a$, but the starting range becomes longer according to the increase of $2a$ and the decrease of u_0. Moreover, when the condition of boundary layer in the case of type I is compared with that of type II, it is shown that they are in the almost same state, but in the case of type II, both the laminar boundary layer and the main stream
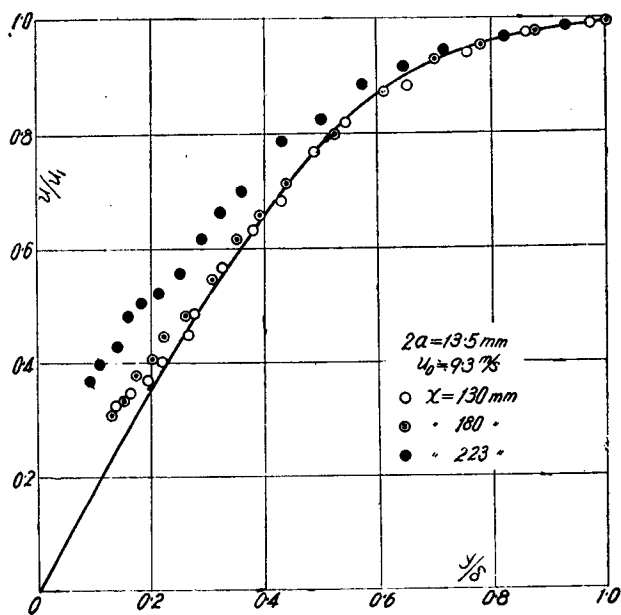
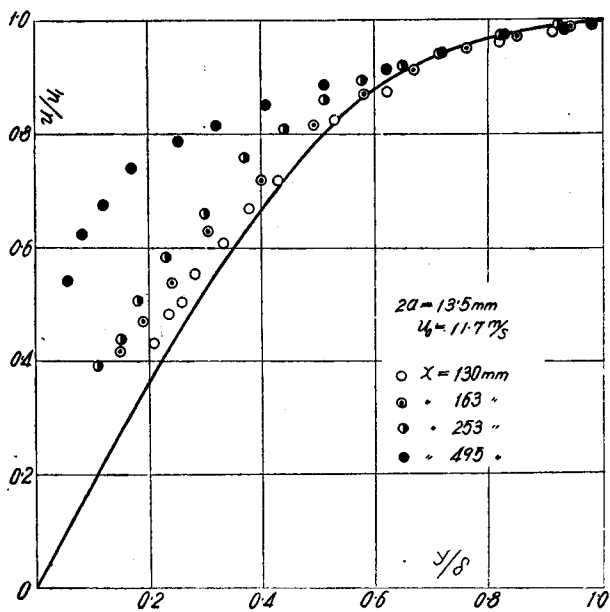Fig. 13.   Velocity distribution
Relation between u/u_1 and y/δ (i)
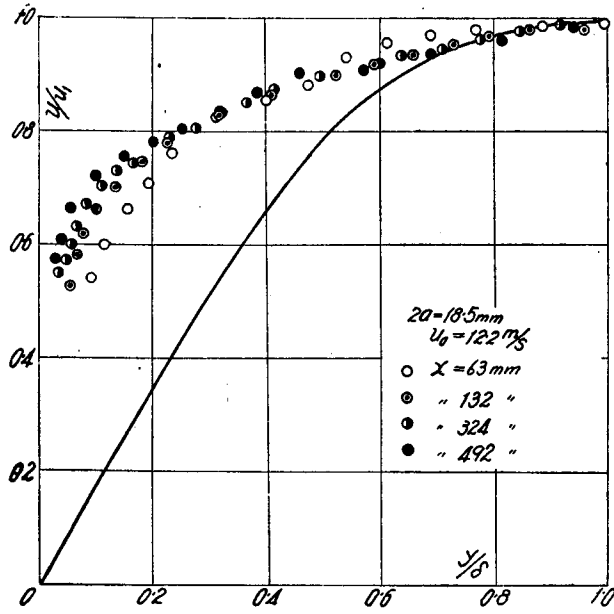

Fig. 14.   Relation between u/u_1 and y/δ (ii)

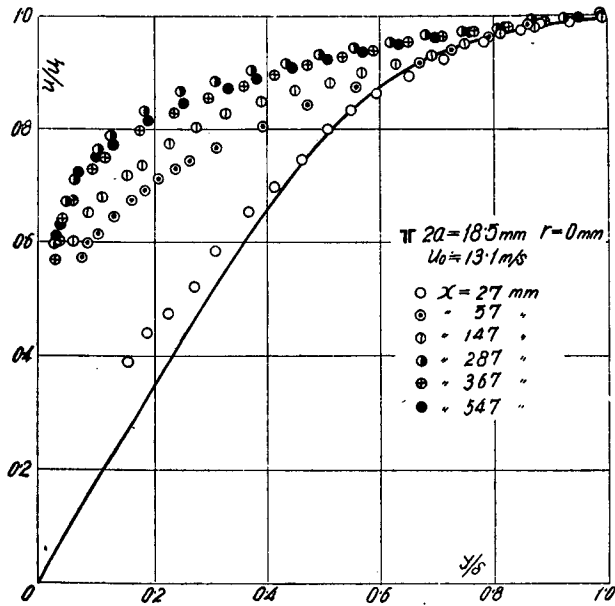Fig. 15. Relation between u/u_1 and y/δ (iii)

Fig. 16. Relation between u/u_1 and y/δ (iv)

contine in a little longer range, and that the boundary layer is rather turbulent in the case of type I. The reason for it, we consider, is that the effect of throttling at the inlet is greater than the effect of the breadth of front edge.

(iii)   Surface Heat Transfer

The results of the local surface heat transfer are shown in Fig. 17 to Fig. 21. Fig. 17 to Fig. 19 show the relation between N_u/R_{ea} and ξ, and Fig. 20 and Fig. 21 show the relation between N_u/R_{ex} and R_{ex}.   Where, $N_u = \alpha x/\lambda$, $R_{ea} = u_0 a/\nu$, $R_{ex} = u_0 x/\nu$, and $\xi = x/(a\ R_{ea})$.

In Fig. 17, the experimental results and theoretical results are compared.   The full line shows the result of theoretical analysis of the laminar heat transfer, but it is modified by taking into consideration the temperature gradient in x direction on the surface of plates[6].   Up to $\xi = 4 \times 10^{-1}$, the experimental results agree well with theoretical result. Furthermore, the chain line shows

Fig. 17.   Relation between N_u/R_{ea} and ξ (i)

the result of the laminar heat transfer in the case of single plate, and its relation is as follows.
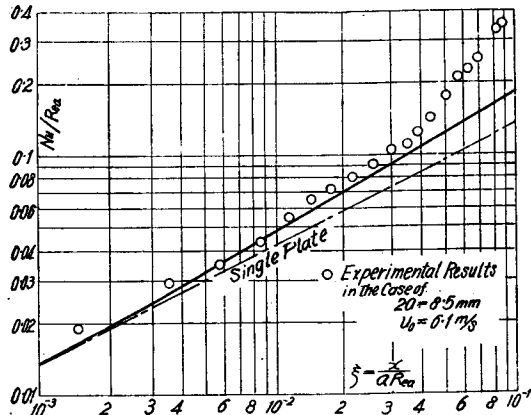
$$N_u = 0.425\,R_{ex}{}^{0.5}\qquad\qquad (22)^{6)}$$

In Fig. 18 & Fig. 19, the broken line is the same as the full line in Fig. 17 and the full lines show the results of turbulent heat transfer, which lines can be shown in the following relation.

$$\frac{N_u}{R_{ea}} = K\,\xi^{0.8}\qquad (23)$$
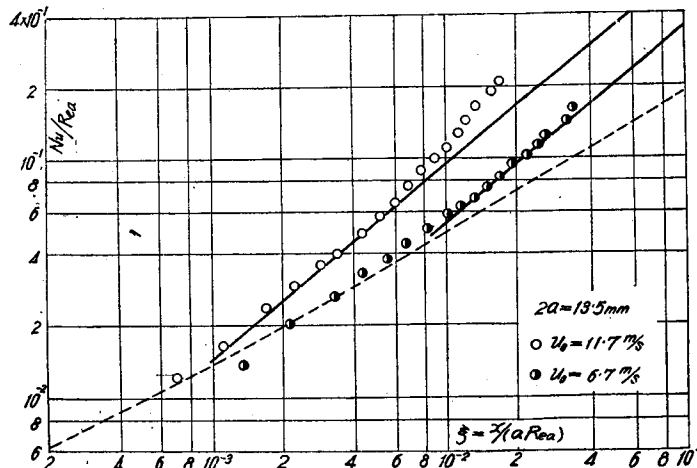
And K is a function of a and u_0.

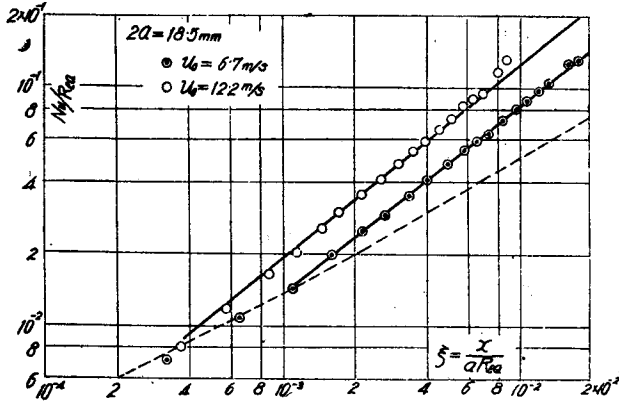Fig. 18.   Relation between N_u/R_{ea} and ξ (ii)

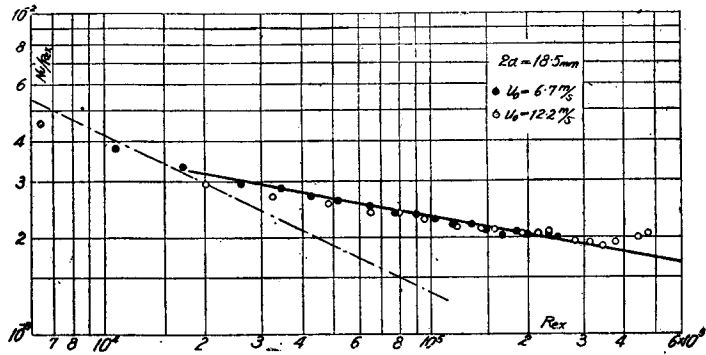Fig. 19.   Relation between N_u/R_{ea} and ξ (iii)

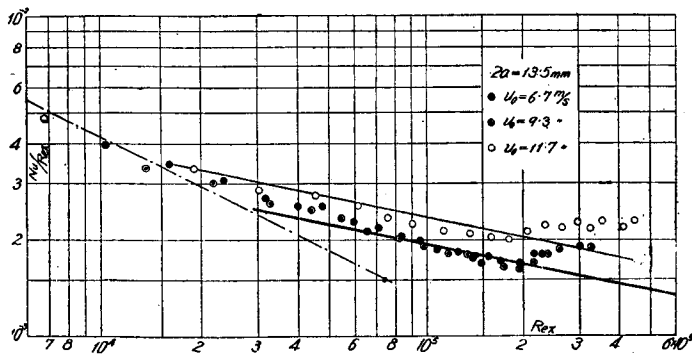Fig. 20.   Experimental results of surface heat transfer (i)

Fig. 21.   Experimental results of surface heat transfer (ii)

The expression which is shown in the relation between N_u/R_{ea} and ξ is convenient in the case of laminar heat transfer, but it is not convenient in the case of turbulent heat transfer, because the results are not unified in a single line. Therefore, we express them, like in Fig. 20 and Fig. 21, by the relation between N_u/R_{ex} and R_{ex}. Fig. 20 is the result in the case of $2a = 18.5$ mm and the full line shows the following relation :

$$N_u = 0.0235\, R_{ex}^{0.8} \tag{24}$$

And the chain line shows the relation of eq. (22). From this figures, it is considered that the starting length shown in the form of Reynold's number is $R_{ex} = 4.5 \times 10^5$ in the case of $2a = 18.5$ mm. Fig. 21 is the results in the case of $2a = 13.5$ mm and the upper full line is the same as that in Fig. 20 and the lower full line shows the following relation :

$$N_u = 0.0194\, R_{ex}^{0.8} \tag{25}$$

And this relation is the same as the results of the turbulent heat transfer in the case of the fluid with very small turbulence flowing along a single plate[7]. As the turbulent heat transfer is influenced a great deal by the turbulence included in the main straem, it is thought that, according to the increase of u_0 and $2a$, the turbulence included in the main straem and the boundary layer increases and, consequently, the surface heat transfer is improved. Moreover, the Reynolds' number showing the starting length is $R_{ex} = 2.5 \times 10^5$ in the case of $2a = 13.5$ mm, and it is $R_{ex} = 1.8 \times 10^5$ in the case of $2a = 8.5$ mm.

4. Conclusion

We performed researches on the heat transfer in the case of parallel plates. At first, the theoretical analysis was carried out on the laminar heat transfer and it is explained that the results of laminar heat transfer can be shown by eq. (20). And this relation agrees well with the results of experiment in the range of laminar boundary layer. Then, various experiments have been carried out mainly in the range of turbulent boundary layer, and the velocity distribution and the statical pressure distribution— consequently the condition of the bundary layer— and the coefficient of the local surface heat transfer have been measured, and the relation between the starting length and the mean velocity or the breadth of a passage has been made clear. From these results, it is made clear that the main stream is converged and accelerated and, on the other hand, the boundary layer is pressed. Therefore, the thickness of the boundary layer becomes thinner than that of a single plate and, consequently, the heat transfer becomes better than that in the case of a single plate. However, the difference between them of the coefficient of surface heat

transfer is not so large as the difference of the thickness of boundary layer. Especially in the range of turbulent heat transfer, it is found that heat transfer is very close to that in the case of a single plate.

Reference

(1) S. Sugawara & T. Satō; The 3 rd Japan National Congress for App. Mech. (1953)

(2) E. Pohlhausen; Z. f. Angew. Math. u. Mech. Bd. 1. (1921)

(3) H. Schlichting; Z. f. Angew. Math. u. Mech. Bd. 14. Ht. 6. (1934)

(4) This method is the same method in the following reference.
     S. Sugawara & T. Satō; Memoirs of the Faculty of Engg. Kyoto Univ. Vol. 14. No. 1. (1952)

(5) H. Blasius; Z. f. Math. u. Physik Bd. 56. (1908)

(6) S. Sugawara & T. Satō; Memoirs of the Faculty of Engg. Kyoto Univ. Vol. 14. No. 1 (1952)

(7) Reference (6) and S. Sugawara, T. Satō and others; Trans. of Japan Soc. Mech. Engrs. Vol. 19. No. 80. (1953)